NREL
NATIONAL RENEWABLE ENERGY LABORATORY

Examination of a Size-Change Test for Photovoltaic Encapsulation Materials

Preprint

David C. Miller and John H. Wohlgemuth
National Renewable Energy Laboratory

Xiaohong Gu
National Institute of Standards & Technology (NIST)

Liang Ji
Underwriters Laboratories Inc. (UL)

George Kelly
BP Solar USA

Nichole Nickel
The Dow Chemical Company

Paul Norum
SolarWorld Industries America

Tsuyoshi Shioda
Mitsui Chemicals, Inc.

Govindasamy Tamizhmani
TÜV Rheinland PTL

Presented at SPIE Optics + Photonics 2012
San Diego, California
August 12–16, 2012

NREL is a national laboratory of the U.S. Department of Energy, Office of Energy Efficiency & Renewable Energy, operated by the Alliance for Sustainable Energy, LLC.

Conference Paper
NREL/CP-5200-54186
August 2012

Contract No. DE-AC36-08GO28308

NOTICE

The submitted manuscript has been offered by an employee of the Alliance for Sustainable Energy, LLC (Alliance), a contractor of the US Government under Contract No. DE-AC36-08GO28308. Accordingly, the US Government and Alliance retain a nonexclusive royalty-free license to publish or reproduce the published form of this contribution, or allow others to do so, for US Government purposes.

This report was prepared as an account of work sponsored by an agency of the United States government. Neither the United States government nor any agency thereof, nor any of their employees, makes any warranty, express or implied, or assumes any legal liability or responsibility for the accuracy, completeness, or usefulness of any information, apparatus, product, or process disclosed, or represents that its use would not infringe privately owned rights. Reference herein to any specific commercial product, process, or service by trade name, trademark, manufacturer, or otherwise does not necessarily constitute or imply its endorsement, recommendation, or favoring by the United States government or any agency thereof. The views and opinions of authors expressed herein do not necessarily state or reflect those of the United States government or any agency thereof.

Available electronically at http://www.osti.gov/bridge

Available for a processing fee to U.S. Department of Energy
and its contractors, in paper, from:

U.S. Department of Energy
Office of Scientific and Technical Information
P.O. Box 62
Oak Ridge, TN 37831-0062
phone: 865.576.8401
fax: 865.576.5728
email: mailto:reports@adonis.osti.gov

Available for sale to the public, in paper, from:

U.S. Department of Commerce
National Technical Information Service
5285 Port Royal Road
Springfield, VA 22161
phone: 800.553.6847
fax: 703.605.6900
email: orders@ntis.fedworld.gov
online ordering: http://www.ntis.gov/help/ordermethods.aspx

Cover Photos: (left to right) PIX 16416, PIX 17423, PIX 16560, PIX 17613, PIX 17436, PIX 17721

Printed on paper containing at least 50% wastepaper, including 10% post consumer waste.

ABSTRACT

We examine a proposed test standard that can be used to evaluate the maximum representative change in linear dimensions of sheet encapsulation products for photovoltaic modules (resulting from their thermal processing). The proposed protocol is part of a series of material-level tests being developed within Working Group 2 of the Technical Committee 82 of the International Electrotechnical Commission. The characterization tests are being developed to aid module design (by identifying the essential characteristics that should be communicated on a datasheet), quality control (via internal material acceptance and process control), and failure analysis. Discovery and interlaboratory experiments were used to select particular parameters for the size-change test. The choice of a sand substrate and aluminum carrier is explored relative to other options. The temperature uniformity of ±5°C for the substrate was confirmed using thermography. Considerations related to the heating device (hot-plate or oven) are explored. The time duration of 5 minutes was identified from the time-series photographic characterization of material specimens (EVA, ionomer, PVB, TPO, and TPU). The test procedure was revised to account for observed effects of size and edges. The interlaboratory study identified typical size-change characteristics, and also verified the absolute reproducibility of ±5% between laboratories.

Keywords: material characteristics, quality assurance, shrinkage, polymer

1. INTRODUCTION

The polymeric materials used for encapsulation within flat-panel photovoltaic (PV) modules typically possess a built-in stress that is later released when the film is heated during the thermal processing (*e.g.*, lamination) used in module manufacturing. Stress-induced size-change for the encapsulation could displace the cells (for crystalline silicon [c-Si] modules), cell interconnects (*i.e.*, "ribbons," for c-Si modules), and bus bars (for c-Si and thin-film [TF] modules). The possible immediate consequences of size change could therefore include: broken solder joints (electrical opens for c-Si), spurious electrical contacts (electrical shunts for c-Si, including cell-to-cell connections and ground faults), cracked cells (for c-Si), residual stress and subsequent delamination (for all PV), and void formation within the encapsulation (for all PV). The long-term effects of encapsulation size-change on PV module performance and reliability are unknown. The short-term effects are expected to exacerbate with the added influence of field deployment.

The goal of this group within the International Electrotechnical Commission (IEC) Technical Committee 82 (TC82) on PV Working Group 2 (WG2) on modules was to create a material-level test standard to assess the change in linear dimensions of sheet encapsulation products. The purpose of the standard is to aid material manufacturers and module manufacturers in performing material acceptance, process development, design analysis, and failure analysis. No "pass" or "fail" criteria are assigned for the proposed test procedure; rather, it is intended to be used for quality control or datasheet reporting.

Certain key considerations were identified during the development of the standard. First, a method was sought that imparted a minimal friction during the test. This requirement contributes to the standardization of the test. For example, friction between a glass/polymer interface may not be repeatable (based on the choice of materials, their surface preparation, and the influence of the ambient environment). The surface energy of glass can vary significantly in the manufacturing and testing environments based on ambient moisture, contamination, and its chemical integrity (corrosion). The composition of the glass itself may also be difficult to control, because the same glass product, produced by the same manufacturer, can acquire residual compositional content from intermediate batches of different glass products. Separately, size change occurring when friction is present is difficult to interpret. The interpretation of the size change for a glass substrate could be compounded by its surface energy, surface chemistry, and surface roughness. Consider also that the interpretation (which may include stress/strain varying through the thickness of the encapsulation) would be difficult to verify through other methods. So, based on the considerations of repeatability and interpretation, a procedure was sought that introduces the least uncertainty in characterizing the *maximum* representative change in linear dimensions.

Several lesser characteristics were desired for the method, including that it be fast, simple, compact, safe, and makes use of standard laboratory (or other commonplace) equipment. Many of these traits would make the method readily amenable to quality control in a manufacturing environment.

Existing tests examining size change in polymeric sheet materials include: ISO 11501 [1], ASTM D1204 [2], and ASTM D2732 [3]. ISO 11501 describes the determination of the dimensional change before and after baking in a kaolin bed located within an oven. Aspects of ISO 11501 that could not be agreed upon within WG2 include: 1) the use of a kaolin substrate, *i.e.*, unstandardized material, and 2) the specified test chamber size, *i.e.*, 120 mm x 120 mm, which could prohibit the simultaneous examination of multiple samples. ASTM D1204 describes the determination of the dimensional change before and after baking within an oven between heavy paper sheets (dusted with talc powder). Concerns related to ASTM D1204 identified within WG2 include the possible adhesion to the paper (which may not be adequately prevented by a thin layer of talc for specimen materials with intended adhesive characteristics), as well as the heat transfer to the specimens (where the paper may affect the heat flux, providing a time-temperature history different from that in a PV laminator). ASTM D2732 describes the determination of the dimensional change before and after submersion in a heated liquid bath, *i.e.*, ethylene glycol, glycerine, or water. Issues related to ASTM D2732 include the: a) test temperature, b) required cross-linking for thermoplastic materials, c) melting of thermoplastic materials, and d) subsequent handling of the specimens.

(a) The method must characterize non-traditional encapsulation materials at their intended processing temperature (*e.g.*, some may be processed at the temperature of 165°C) in addition to ethylene-co-vinyl acetate (EVA, which may be laminated at ≥132°C). In comparison, the boiling points of ethylene glycol, glycerine, and water are 197°, 290°, and 100°C, respectively. Although ethylene glycol and glycerine may be used to examine contemporary encapsulation products, water is limited by its boiling point and therefore would not be capable of providing the required temperatures. The density of ethylene glycol and glycerine are 1.11 and 1.26 $g \cdot cm^{-3}$, meaning that many polymers would float at the top of the bath. Water (even at 80°C) may induce size change in EVA (which melts at ~65°C [5]); however, the size change associated with the melt transition may not be complete, depending on the time-temperature history of the submerged specimen.

(b) Water is not expected to invoke cross-linking (with subsequent strain), which occurs above 120°C. Because both thermal processing and chemical cross-linking may produce measurable size change for EVA, the test procedure is expected to examine the effects of both.

(c) Although the formulated EVA used in PV modules will cross-link to a final (fixed) size, many other encapsulation products are thermoplastics not subject to fixed final dimensions. That is, the thermoplastic materials would be examined in their molten state.

(d) Submersion characterization is complicated by the unloading of the specimen from the liquid bath. The handling of the specimen (typically achieved using a wire-mesh basket) to extract and cool the specimen may introduce additional shape change. Handling could be aided by injecting cool liquid into the bath to reduce its temperature prior to specimen removal. Unintended size change from handling would be difficult to avoid, particularly for molten thermoplastic materials.

The method developed within WG2 is based on a procedure used internally at BP Solar. The specific task group for the standard was formed in the autumn of 2010. Discovery experiments supporting the initial draft of the standard were conducted in the spring and summer of 2011. An interlaboratory study was performed in the summer and autumn of 2011. A test procedure was then submitted to the IEC as a new proposal (NP) in the autumn of 2011. A revised method is expected to be submitted to the IEC in the autumn of 2012 or spring of 2013.

The goal of the described experiments was to support the development of a standardized test procedure that can be used to evaluate the maximum representative change in linear dimensions of sheet encapsulation products (resulting from their thermal processing, occurring during the manufacture of a PV module). Discovery experiments were used to examine issues, including the choice of "substrate," uniformity of temperature, specimen size-effect, and specimen edge-effects. An interlaboratory study was conducted to assess the reproducibility of measurement between different laboratories. The combined experiments were also intended to identify potential issues. The results of the discovery and interlaboratory study were used to better define and improve the test procedure.

2. EXPERIMENTAL*

2.1 Specimens

Specimens examined in this study include sheet products composed of: EVA, poly(ethylene-co-methacrylic acid metal salt) ("ionomer"), polyvinyl butyral (PVB), thermoplastic polyolefin (TPO), and thermoplastic polyurethane (TPU). To date, EVA certainly has the most substantial legacy of use in PV modules. A peroxide is typically added to the PV EVA formulations to cross-link the material during module lamination; peroxide-containing commercial formulations were examined during the development of this test standard. For the purpose of the study, the specimens were used as received from their manufacturer and were not subject to pre-conditioning (other than as prescribed for storage). Specimens were cut to the size of 100 mm x 100 mm (using scissors or a blade) for the test. After cutting, the specimens were marked with a marker to show the machine-extrusion direction (MD), along the length of the roll, and transverse direction (TD), across the width of the roll. The test procedure [6] specifies that a minimum of six replicates be examined. The procedure also provides guidance for its application in industry, *e.g.*, the preferred location for sampling from a roll of material.

2.2 Test procedure

The initial size (in at least five locations per direction) and thickness (in at least three locations) must first be measured (*e.g.*, using a ruler or micrometer, respectively) for the specimens. An accuracy of 0.5 mm is required for the size measurements and an accuracy of 0.01 mm is required for the thickness measurements. Next, a sheet of aluminum foil is placed on a heated platen (a circulating oven is presently identified for the test, instead of a heated platen). A layer of sand (about 2–4 mm thick) is then placed on the aluminum foil. (The choice of sand was not specified at the time of the discovery experiments.) The procedure then calls for the platen to be equilibrated to the encapsulation manufacturer-designated processing temperature. A specimen is then placed on the equilibrated sand substrate. After the designated duration (300 s), the Al foil is removed from the platen and allowed to equilibrate to ambient temperature. The final size is then measured for each of the directions. The size change, ΔL, is determined from Equation 1 in units of percent, where L represents the size {m} and the subscripts $-i$ and $-f$ refer to the initial and final conditions, respectively. From the six different samples, the maximum size change (the maximum of the 30 measurements) and corresponding difference (the maximum of the 30 measurements minus the minimum of the 30 measurements) are reported for each direction. The average size change and corresponding standard deviation (of the 30 measurements) are also reported for each direction.

$$\Delta L = 100 \cdot \frac{L_f - L_i}{L_i} \tag{1}$$

2.3 Additional characterization

The size change was characterized as a function of time for the different encapsulation materials. Here, each specimen was photographed (every 20 s) using a tripod-mounted camera (40D, Canon Inc.). The change in size could be determined from a ruler, located adjacent to the specimen. Measurements were obtained from the middle and near the corners of each specimen, *i.e.*, three measurements in both the machine and transverse directions. The accuracy of the measurements was on the order of 1 mm, *i.e.*, ±1%.

Temperature characterization of the substrate and specimens was performed using infrared thermography. For example, a ThermaCAM SC640 camera (FLIR Systems Inc., which operates at wavelengths from 7.5 to 13 μm) is capable of resolving temperature within 0.06°C. A Ti32 (Fluke Corp.) was also used in the experiments. Sand is a high-emissivity material, readily enabling thermography. Although the emissivity of sand may exceed 0.9 (particularly when wet) [7], the value of 0.90 was used in the approximate measurements (with an accuracy on the order of 2°C).

Additional characterizations were performed to assess size and edge effects. The appropriateness of the specimen size and measurement locations was examined by performing measurements at the edges and interior. The interior measurements were assessed at 40, 60, and 80 mm (in addition to 100 mm). The measurements were performed on a site indicated (using a marker) on each specimen prior to the test.

---

*. Instruments and materials are identified in this paper to describe the experiments. In no case does such identification imply recommendation or endorsement by NREL or NIST.

3. RESULTS AND DISCUSSION

3.1 Substrate temperature and its uniformity

The substrate originally proposed for use in the test method was glass, covered with a 2–4-mm-thick layer of talc powder to prevent friction at the glass/encapsulation interface. A glass/talc substrate was originally used at BP Solar. In discovery experiments, the temperature uniformity of a glass substrate was examined using thermography. Glass may be readily characterized using thermography (here, using the emissivity of 0.95 [8]) because of its high emissivity at the wavelengths examined. Low-iron, soda-lime float-glass substrates (as used in PV modules, 125 mm x 125 mm in size) demonstrated poor temperature uniformity (>20°C). Temperature heterogeneity was understood to result from curvature of the glass (glass is seldom perfectly flat), which can be further accentuated by temperature (the concavity of glass typically increases with temperature).

The substrate was then selected to consist of an aluminum foil base layer (which acts as a heat spreader to improve temperature uniformity), topped with a layer of sand (where the sand reduces friction at the aluminum/encapsulation interface and also weights the aluminum to improve its thermal contact to the heated platen). Figure 1 shows corresponding (a) optical and (b) thermographic images of the apparatus (sand/Al foil/platen). A PC-620 heated platen (Corning Inc.) with a 25 cm x 25 cm stage is used in Figure 1. The set temperature for the platen was 132°C. The measured surface temperature is indicated in Figure 1(b) for a uniform array of locations. The average surface temperature for a 10 cm x 10 cm region within the center of the sand was 125±3°C (one standard deviation [s.d.]); the maximum and minimum surface temperatures within the same test region were 133° and 113°C, respectively. Some irregularity in the temperature of the sand likely results from thickness variation in the figure (where partially exposed aluminum would readily compromise thermography). An aluminum foil is difficult to accurately characterize because of its low (<0.1) emissivity [8]. A 4°–8°C temperature range was typically observed for well-manicured sand. Localized variation could be observed, for example, if the sand was irregularly graded with a straight edge.

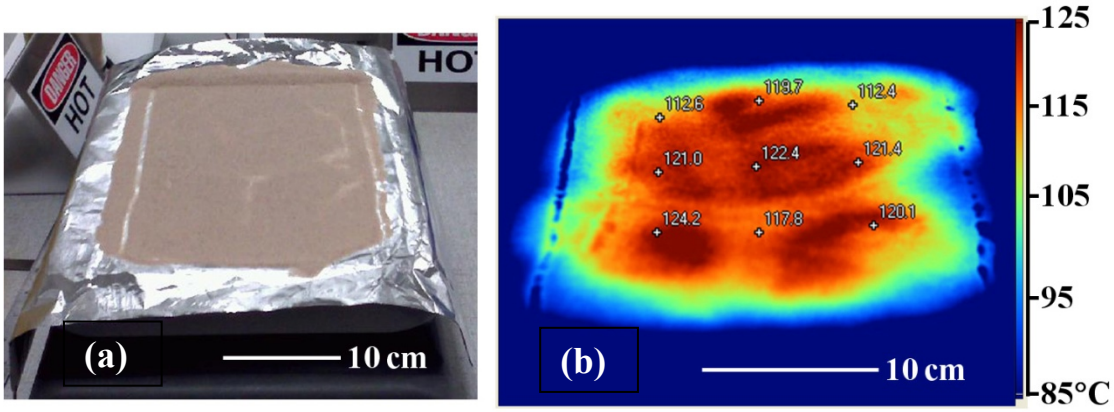

Figure 1: Corresponding (a) optical and (b) thermographic images of the apparatus (platen/Al foil/sand). The measured surface temperature is indicated for a uniform array of locations in (b).

The thermography characterization was performed to quantify the temperature variation across an Al foil/sand substrate. The characterization importantly identifies a difference between the set temperature for the platen and the surface temperature of the sand. A 5°C range is anticipated for a skilled operator. This, however, does not take into account a temperature gradient that may exist between the heated platen (controlled to a specified temperature) and the top surface of the sand (which is cooled by the ambient environment).

3.2 Choice of substrate carrier

As shown in Figure 2, a follow-up experiment was conducted to compare the use of different carriers for the sand "substrate." Aluminum foil, kraft paper (the release liner paper often used in rolls of EVA), and a stainless-steel plate (SS plate) were alternately placed on top of the same heated platen and then covered with sand. At least 20 replicates of the different EVA_1 ("unbalanced") and EVA_2 ("balanced") formulations were examined using the test method. Error bars (2 s.d.) are shown in Figure 2. The results for the unbalanced EVA were similar between the different carriers, *i.e.*, ~17% size reduction for the MD and ~3% size reduction for the TD. The results for EVA_2 were also similar between the different carriers, *i.e.*, ~6% size reduction for the MD and TD. EVA_2 had been

specifically engineered by its manufacturer to reduce and balance the size change occurring during lamination. The size change is consistently less for the SS plate, but not outside the range of variation for the experiment.

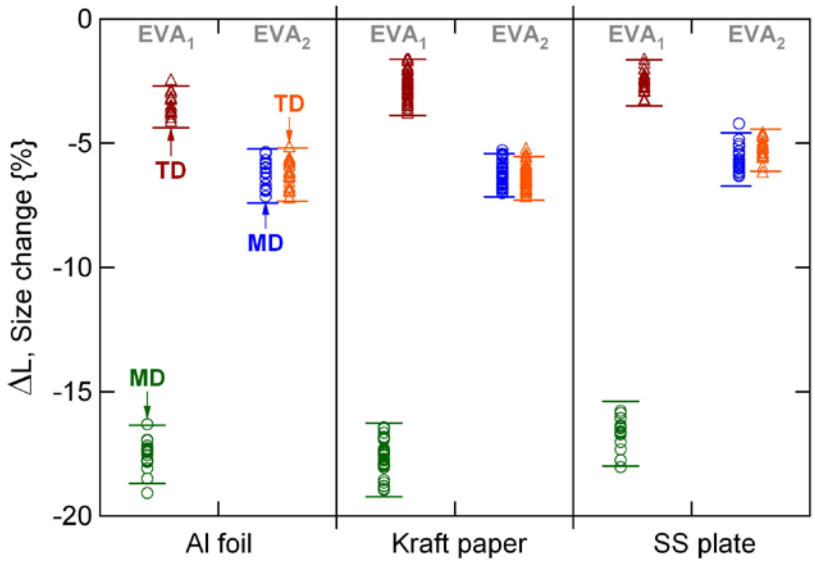

Figure 2: Comparison of carrier/sand substrates for the EVA_1 (unbalanced) and EVA_2 (balanced) formulations. Results are indicated for the machine-extrusion direction (MD) and transverse direction (TD). The error bars are shown for two standard deviations.

The results for Al foil, kraft paper, and the SS plate are comparable and suggest no overt difference. This implies that the size-change behavior is accommodated by the sand substrate itself, and not the carrier. The lesser size-change for the SS (if applicable) may result from the thermal capacitance, lesser thermal conductivity, and thermal resistance of the plate of finite thickness. Because the results were similar for the different substrate carriers, Al foil was chosen because of the greater thermal conductivity and malleability of Al (both characteristics are expected to minimize the thermal contact resistance at the surfaces of the carrier, thereby improving the temperature uniformity of the sand).

3.3 Confirming the appropriate test duration

Size change with time is shown in Figure 3, Figure 4, and Figure 5 for EVA_1 (the unbalanced EVA formulation), EVA_2 (balanced), and TPO, respectively. Error bars are shown in the figures for the maximum and minimum of the three measurements (obtained along the edge at the corner, middle, and corner) from each of the individual specimens. The "corner" measurements were made along the edge, about 5 mm from the true corners of the specimens. The relative size and corresponding sample directions are shown in the insets of the figures, before (dashed) and after (solid) the test. The dashed and solid profiles are approximately to scale based on photographs of the specimen, but do not convey the details including curvature or irregularity at the edges. The results at 600 s are summarized in Table 1 for Figure 3, Figure 4, and Figure 5, as well as some materials that are not shown (PVB, TPU, and an ionomer). Except for EVA_2, the MD demonstrated the greatest size change. Several of the materials (the PVB, TPO, TPU, and ionomer thermoplastics) changed size by shrinking in the MD, but expanding in the TD. The majority of the size change occurred within the first 200 s of all of the experiments summarized in Table 1. As in Figure 3, Figure 4, and Figure 5, some minor size change continued to occur for all of the specimens at 600 s.

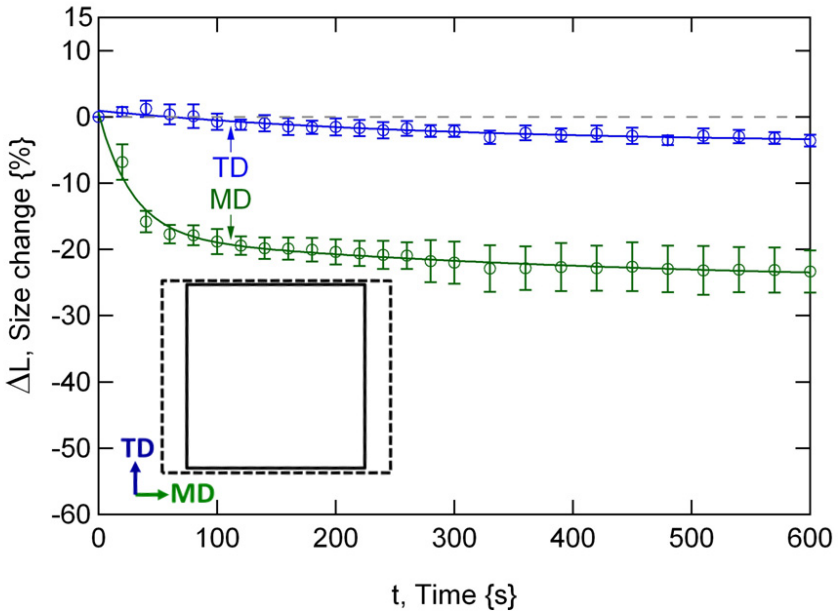

Figure 3: Size-change results for "EVA_1," the unbalanced EVA formulation. The relative size and corresponding sample directions are shown in the inset before (dashed) and after (solid) the test, based on photographs of the specimen. Error bars are shown for the maximum and minimum of the measurements, obtained along the edge of the specimen at the corner, middle, and corner.

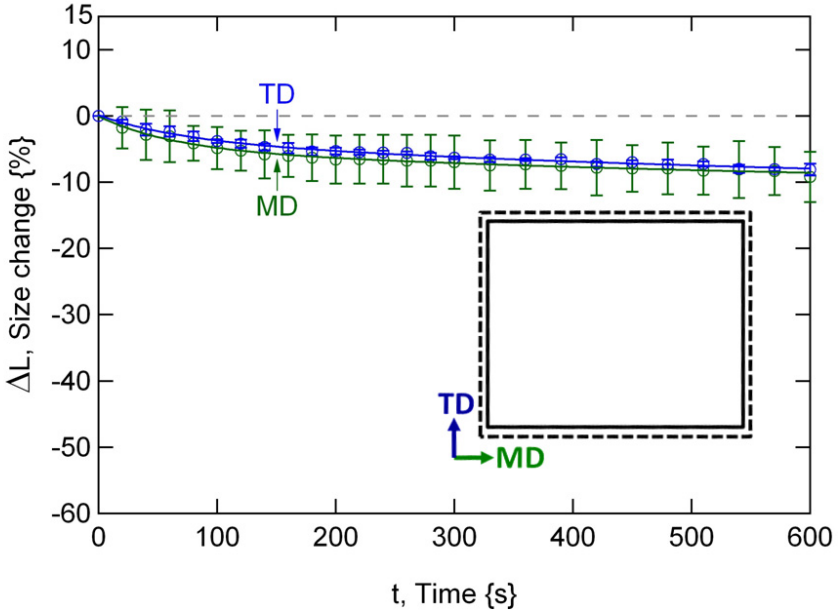

Figure 4: Size-change results for "EVA_2," the balanced EVA formulation. The relative size and corresponding sample directions are shown in the inset before (dashed) and after (solid) the test, based on photographs of the specimen.

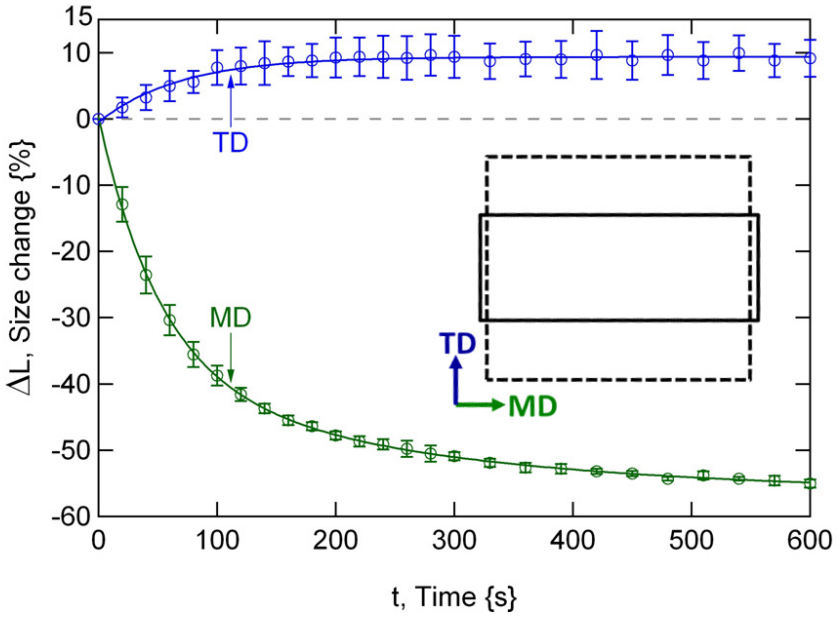

Figure 5: Size-change results for TPO. The same range and scale for ΔL is shown in Figure 3, Figure 4, and Figure 5. The relative size and corresponding sample directions are shown in the inset before (dashed) and after (solid), based on photographs of the specimen.

Table 1: Summary of results for the time characterization experiments, including Figure 3, Figure 4, and Figure 5.

	MATERIAL					
GREATEST SIZE-CHANGE {%}	EVA_1	EVA_2	PVB	TPO	TPU	Ionomer
MD	-23	-9	-31	-55	-38	-35
TD	-4	-8	+12	+9	+12	+9

Figure 3, Figure 4, and Figure 5 confirm that much of the size change for the various encapsulation materials occurs within 5 minutes. The rapid size change is true for both thermosets (*i.e.*, EVA) and thermoplastics (ionomer, PVB, TPO, and TPU). A small amount of size change continues even at 10 minutes. This may correspond to continued cross-linking (for EVA), specimen/substrate interaction, gravitational effect, or thermal equilibration. In principle, the thermoplastics should be free to flow within their melt state, identified in Ref. [5].

Figure 3, Figure 4, and Figure 5 serve as examples of the range of behavior that might be expected in contemporary encapsulation products. This includes a balanced size change (for EVA_2, where a 10% shrinking is typical), or a more substantial and unbalanced size change (for TPO, where the maximum of 55% shrinking was observed in this study). To clarify, some materials (including ionomer, PVB, TPO, and TPU in this experiment) shrink in one direction and expand in the other. The greater shrinking observed in the machine direction is expected, based on the process (extrusion) typically used to manufacture the materials. The implications for the stress in a module resulting from the observed size change are unclear, but might be understood using finite element analysis. To explain, a threshold size-change for problematic behavior (*e.g.*, interconnect damage in c-Si modules) may exist. Further, the size-change associated with processing the encapsulation must be taken into account by the manufacturer, *e.g.*, when sizing the amount of encapsulation and strain relief to use in modules. Several of the products examined here were probably not optimized to reduce size-change, as vendors were likely unaware of the issue. It is expected that the substantial and unbalanced size-change could be reduced for these products using processing methods, *e.g.*, annealing.

3.4 Specimen size-effect

Measurements were obtained from the specimen interior to help assess a specimen size-effect, and therefore, the appropriateness of the size specified in the standard. The results of the size-specific measurements are shown in Figure 6 for EVA_1 (the unbalanced formulation). Error bars (2 s.d.) are shown in Figure 6 for the five specimens examined. The left inset of Figure 6 includes a photograph of one of the EVA_1 specimens, and the right inset shows

the measurement location and naming scheme for the specimens. For example, the measurement from locations *a* to *a*' occurs across the machine direction (nominally 100 mm), at the edge of the specimen. As another example, the measurement from locations *I* to *I*' occurs within the transverse direction (nominally 40 mm), near the middle of the specimen. In Figure 6, a monotonic trend is observed for EVA_1 in the MD. The shrinking increases with the size of the sample region for EVA_1, as observed for the ionomer, PVB, and TPO in both the MD and TD (not shown). In contrast, the size change varies significantly with the measurement location for EVA_1 in the TD, Figure 6. Here, the shrinking is greatest at the edge of the specimen. A similar behavior was observed for EVA_2 (in both the MD and TD), but was not observed of the other encapsulations.

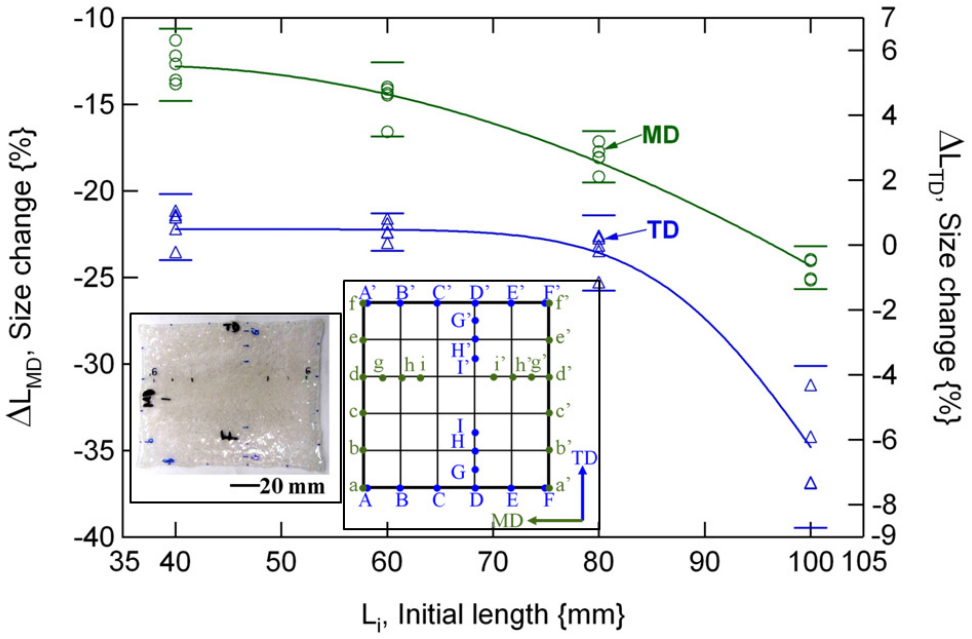

Figure 6: Size-specific results for "EVA_1" (unbalanced). A photograph of one of the specimens is also shown (inset, left); the measurement location and naming scheme is shown for the same specimen orientation (inset, right).

Figure 6 importantly identifies a modest size effect that occurs for all of the encapsulation materials examined. A linear fit could be applied for EVA_1 in the MD, with perhaps a better fit for the ionomer, PVB, and TPO (both directions, not shown). The size effect itself is not overly concerning, because the size of the specimens is standardized in the proposed test procedure. The size of 100 mm is chosen for the standard based on practical convenience—as opposed to the entire width of the roll, which would be more difficult to handle, require larger test equipment, and may even more readily demonstrate size- and edge-related heterogeneity. The results in Figure 6 simply reaffirm the need to standardize the size of the specimens, thereby standardizing the nominal dimension of the measurement. The causes of the size effect could include: friction (from sand), stretching occurring when the specimens were cut to size, uneven and rapid cooling at the end of the test, and heterogeneous stress incurred during manufacturing. For friction to be a significant contributing factor would imply that the friction for the sand substrate is minimal, but not zero (as would ideally be the case).

3.5 Edge effect (location of measurements)

The measurement location scheme used to examine size effect, Figure 6 (inset, right), was also used to examine edge effect. The specimen profiles for EVA_1 (the unbalance formulation) are shown in Figure 7, with error bars (2 s.d.) for the five specimens examined. To clarify, the measurements were performed at locations along the edge of the specimens, specifically including their corners. The final shape for one of the EVA_1 specimens is shown in Figure 6 (inset, left). In Figure 7, the least size change for the specimens is observed at the corners; the greatest size change occurs at the middle. A similar profile was observed for EVA_1, EVA_2, ionomer, and TPO, *i.e.*, $\Delta L_{DD'} > \Delta L_{AA'}$. The opposite profile was observed for PVB, where the corners changed size more than the middle, *i.e.*, $\Delta L_{AA'} > \Delta L_{DD'}$. Although only the profiles for EVA_1 are shown, a minor effect (ΔL on the order of a few percent) is evident in all the materials.

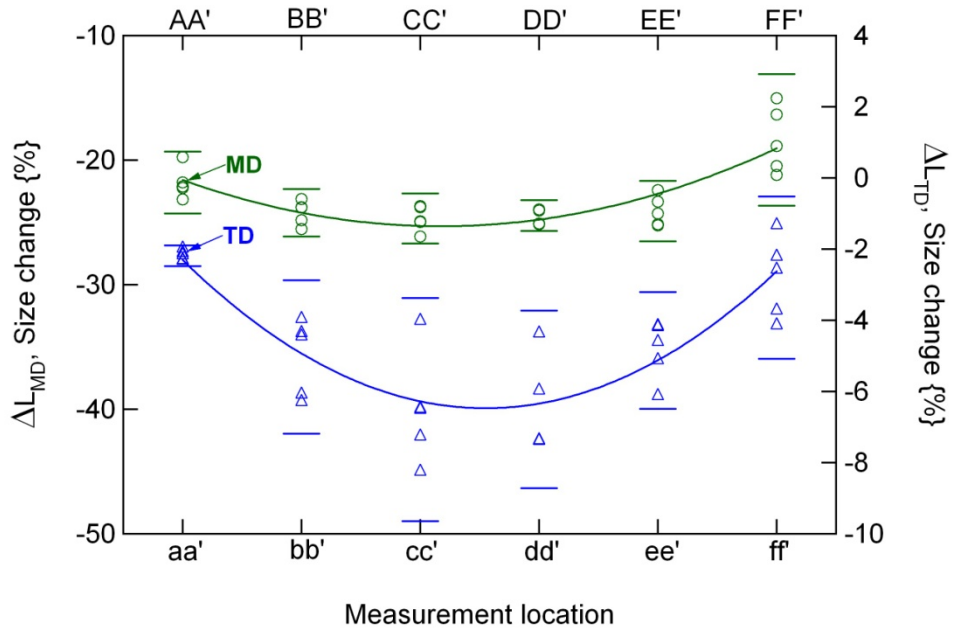

Figure 7: Location-specific results showing the profile at the edges of "EVA_1" (unbalanced). The details of the measurement locations are identified in Figure 6 (inset, right).

The characterization summarized in Figure 7 confirms that a minor edge effect is present for all of the materials examined. The observed size and edge effects suggest the need to standardize the measurement by specifying the number and the location of the measurement sites. For example, an odd number of measurements can be used to examine the corners and middle of the specimen. The size change at the tips of the corners, however, is not considered representative of the bulk material. The revised standard therefore specifies to obtain measurements at least 1 cm away from the corners (implying an approximate spacing of 1, 2, 2, 2, 2, and 1 cm along the edge of the specimen). Because the specimens may distort as a result of the test, measurements ambiguity is minimized by marking the measurement locations with a felt-tipped marker, for use before and after the test.

A similar edge effect may exist within the roll of encapsulation from which the specimens are obtained, based on the manufacturing process used to produce the material. Because an edge effect may exist within the encapsulation roll, the sampling (location) from within the roll should be specified. Therefore, the test procedure will specify to obtain specimens at a location away from the outside edges of the roll. Some users may wish to apply the test procedure for other purposes, such as verifying the homogeneity of the material across the width of the roll of encapsulation. In such cases, it makes sense to sample material from other locations within the roll.

3.6 Treatment of out-of-plane curvature

Because the proposed test procedure is intended to examine change in linear dimension, it does not treat out-of-plane deformation. For example, the shape of an early-generation ionomer product after a 5-minute test is shown in Figure 8(a). The original profile of the specimen is outlined (dashes) in the figure; arrows are used in the figure to identify the edges of the specimen after the test. A size change for the ionomer on the order of -50% in the MD and +15% in the TD was determined for the material. The curled final shape likely results from a significant through-thickness-oriented strain gradient present in the material before the test. With knowledge of the result in Figure 8(a), the size change (including the out-of-plane curvature) would likely be significantly improved through the engineering of the manufacturing process. Because the ionomer material is relatively rigid and it becomes frozen in place at the ambient temperature (Table 2), it is not practical to uncurl the specimens for measurement at the end of the test. For the manufacturer to quantify and therefore be able to reduce the size change of an encapsulation product, how can size change be examined for materials with a significant through-thickness strain gradient?

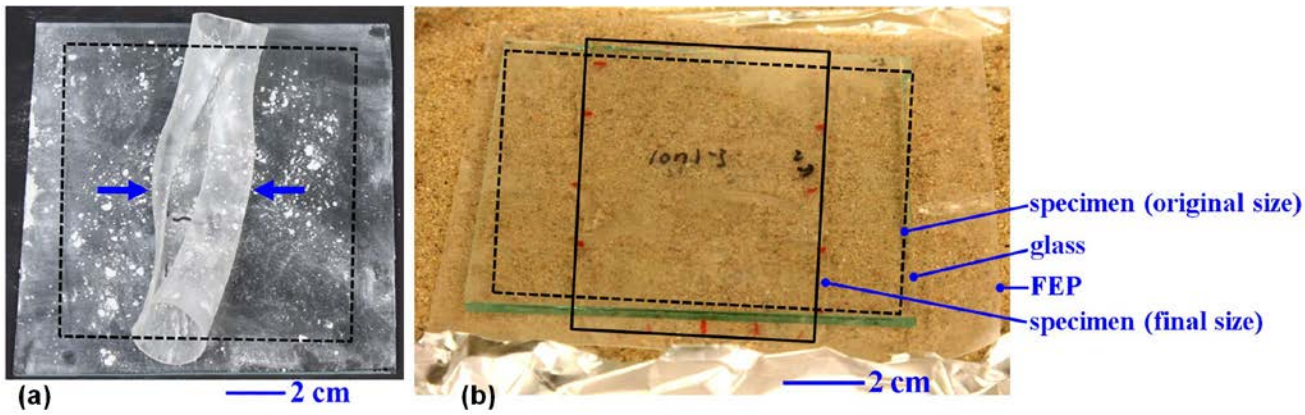

Figure 8: Ionomer specimens: (a) photograph of the final shape for an uncovered specimen, (b) photograph of specimen covered with FEP and weighted with glass. The original profile of the specimen is outlined (dashes); the final shape is shown with a solid border.

One solution method explored was to cover the ionomer with Teflon fluorinated ethylene propylene (FEP) resin sheet, as shown in Figure 8(b). A piece of glass is used in Figure 8(b) to provide additional weight and maintain the planarity of the specimen. The original profile of the specimen is outlined (dashes). Figure 8(b) also shows a border (solid) that outlines the irregular final shape of the specimen. In Figure 8(b), the specimen is located on a sand substrate, whereas a substrate coated with talc powder was used in Figure 8(a). However, the weighted, low-friction cover material in Figure 8(b) was confirmed to affect the result, Table 2. Therefore, the size-change final profile of the specimen in Figure 8(b) is only approximate and will vary with the mass of the cover used. In situations like that shown in Figure 8(a), a minimal modification (least likely to affect the in-plane deformation) is preferred, *e.g.*, just the Teflon cover in Figure 8(b) may prove sufficient to prevent out of plane deformation. The use of a low-friction cover is identified here as a possible method to examine materials with a known through-thickness strain gradient. An improved method that may be used to standardize the measurement of specimens prone to out-of-plane curvature would benefit the test procedure.

3.7 Results of interlaboratory study

An interlaboratory study was conducted at eight participating laboratories using (six) replicates of different test materials (EVA_1, EVA_2, PVB, TPO, and ionomer), where the replicates were all cut from the same roll of material. Each specimen was examined once because the test cannot be repeated. Even though the interlaboratory study was performed according to the procedure originally submitted to the IEC, certain limitations apply to the study. Some of the details of the experiment—such as the difference between the T_{set} for the heater device and the surface temperature of the sand—motivated revision of the standard after the results of the interlaboratory study were examined. Also, some participants used a heated platen, whereas others used an oven, for the two types of heater devices to be compared. NIST specifically used ASTM C778 sand [4].

The results of the interlaboratory study are summarized in Table 2. The data provided include the maximum size change (of the 30 measurements in each direction for the six specimens examined), as well as the difference (maximum minus the minimum of the 30 measurements). As in Figure 3 and Figure 5, all of the participating laboratories identified a greater size change in the machine direction than in the transverse direction for EVA_1, PVB, TPO, and the ionomer. As in Figure 4, the direction of greater size change was not readily distinguished for EVA_2. The results were reproducible between participating laboratories—within ±5% of the absolute size change (based on the measured L_i values), although varying by up to 40% of the relative size change (based on the ΔL results from Equation 1). The results for the ionomer proved even less reproducible between the laboratories. Here, the out-of-plane curvature and the corresponding methods (as in Figure 8[b]) used to characterize the specimens resulted in increased variability.

The set (T_{set}) and phase-transition temperatures are also identified in Table 2. As in Figure 1, T_{set} for the heater device may differ from the surface temperature of the sand. The phase-transition temperatures include the glass transition (T_g), melt transition (T_m), and freeze transition (T_f) temperatures. The phase transitions were determined using a differential scanning calorimeter (DSC, Q1000, TA Instruments, Inc). The 2-Hz data were taken from the second of two consecutive cycles (from $-100° \le T \le 200°C$) at the rate of 10^0C/min in an N_2 environment. Table 2

identifies that most of the materials (except PVB) were examined in their melt state. The PVB is, however, significantly softened at the test temperature used in the experiment [5].

Table 2: DSC measured phase-transition temperatures results and (size-change) data from the interlaboratory study. The greatest value and the corresponding difference (based on the maximum and minimum) are provided.

	MATERIAL									
ATTRIBUTE	EVA_1		EVA_2		PVB		TPO		Ionomer	
T_{set} {°C}	132		132		160		140		165	
T_g=T_α {°C}	-33		-33		15		-44		26	
T_m {°C}/T_f {°C}	55/35		55/35		N/A		60/55		86/46	
	MAXIMUM SIZE-CHANGE PER DIRECTION, GREATEST (AND DIFFERENCE)									
PARTICIPANT	MD	TD	MD	TD	MD	TD	MD	TD	MD	TD
BP Solar USA	-23.6 (5.2)	-1.4 (0.7)	-8.9 (2.9)	-6.1 (1.4)	-41.2 (7.5)	14.8 (2.7)	-48.7 (1.9)	7.7 (1.9)	-56.2 (7.4)	27.2 (8.3)
Dow Chemical	-28.0 (8.0)	-9.0 (6.0)	-12.0 (4.0)	-13.0 (5.0)	-42.7 (3.0)	14.6 (4.6)	-55.0 (2.2)	8.0 (2.0)	-65.7 (13.2)	29.5 (14.6)
Mitsui	-29.0 (6.4)	-7.5 (7.0)	-13.0 (7.0)	-10.5 (4.5)	-33.7 (3.7)	11.7 (0.3)	-49.0 (3.5)	7.5 (0.5)	-51.2 (N/A)	17.1 (N/A)
NIST	-32.2 (17.2)	-8.3 (8.7)	-12.9 (10.1)	-12.2 (7.2)	-43.6 (13.2)	16.7 (4.6)	-56.1 (3.2)	10.1 (4.8)	-36.4 (19.9)	17.1 (14.9)
NREL	-25.5 (6.9)	-8.2 (5.0)	-11.0 (1.7)	-10.0 (3.5)	-40.0 (12.5)	14.0 (1.7)	-52.9 (3.3)	13.7 (7.0)	-50.4 (10.5)	16.5 (5.3)
SolarWorld	-30.0 (8.0)	-10.0 (5.0)	-16.0 (8.0)	-14.0 (4.0)	-43.0 (21.0)	17.0 (8.0)	-54.0 (29.0)	7.0 (5.0)	-69.0 (27.0)	30.0 (17.0)
TÜV	-30.1 (11.7)	-5.7 (3.8)	-10.0 (3.6)	-8.1 (3.6)	-44.4 (5.7)	14.5 (2.1)	-56.8 (2.0)	8.0 (3.0)	-87.2 (3.6)	37.6 (8.1)
UL	-23.9 (9.1)	-8.1 (6.2)	-12.5 (6.5)	-12.8 (6.6)	-42.8 (17.2)	11.0 (3.0)	-58.3 (1.9)	8.9 (2.6)	-69.0 (14.6)	30.8 (21.2)

3.8 Choice of oven (or platen)

The data in Table 2 were obtained using a hot plate (*e.g.*, BP Solar, Mitsui) or oven (*e.g.*, NIST, TUV). The experiments at NREL used a hot plate that was surrounded on the sides and top with glass plates (for PVB, TPO, and ionomer) to facilitate achieving T_{set} within the sand (verified using a thermocouple) and to reduce the temperature variability (by reducing convective heat transfer). No obvious trend is observed in Table 2 for the hot-plate vs. oven-heated specimens. The use of a heated platen more closely emulates the application (where industrial lamination machines are heated on one side only). Figure 1 identifies an achievable temperature range (uniformity) of 5°C at the surface for a heated platen, which does not consider other factors, *e.g.*, temperature gradients through the thickness of the sand. Controlled temperature within 5°C is therefore expected for an oven. The use of an oven (or similar heated enclosure) should reduce the variability of the data by limiting heat transfer between the specimen(s) and ambient environment. Arguments considered in favor of an oven include:

- For example, the use of an oven is expected to reduce the difference between the set temperature for the experiment and the surface temperature of the sand. This should also reduce the temperature variability shown in Figure 1(b) that can result from imperfectly raking the sand.
- The thermal capacitance (mass) of an oven should separately aid in maintaining a constant temperature, because the chamber interior should have equilibrated prior to the test. An oven should therefore improve the repeatability of the results, which might only become evident on a much larger number of specimens.
- Circulation within the oven may be used to minimize the temperature recovery resulting from the opening and closing of the oven door, and should aid the transition time for the specimen to its set temperature. The good thermal contact (through the aluminum) between the heated oven and sand carrier should also improve recovery time. Commercial ovens typically use metal shelves (or a metal chamber). The high thermal conductivity or metal components (in addition to the Al foil carrier) should improve recovery time and temperature uniformity.
- The use of an oven may also improve the safety of the test standard, because the heating device consists of a sealable enclosure. The revised version of the standard will therefore specify to use a circulating oven for the test.

4. CONCLUSIONS

A proposed test standard that can be used to evaluate the maximum representative change in linear dimensions of sheet encapsulation products for PV modules (resulting from their thermal processing) was examined using discovery and interlaboratory experiments. Key results include the following:

The use of a sand substrate is advocated to reduce friction (enabling the maximum size change and thereby standardizing the test) and also because it may be used over a wide range of test temperatures. The use of a sand substrate on an aluminum carrier improved temperature uniformity, *e.g.*, relative to a glass carrier. Thermographic characterization suggests that a temperature range as small as 5°C is possible for sand. From the measurements, the use of a circulating oven was specified in the standard for practical reasons (removal of temperature gradient through the sand, elimination of radiative heat transfer, improved recovery time after loading, and safety) that are expected to result in temperature uniformity and temperature stability superior to that of a heated platen.

Many key details related to the test procedure were verified in discovery experiments. The test duration of 5 minutes was found to allow for the majority of size change to occur in a variety of encapsulation materials. Minor size-effect and edge-effect behaviors were observed for a variety of encapsulation materials. The details of the measurement locations and sampling of the specimens were revised in response to these effects. Five evenly spaced, marked measurement sites are used, with two of the sites being at least 1 cm away from the corners of the specimens. Similarly, specimens should be obtained from at least 200 mm from the edge of a roll. Although the use of a low-friction cover was given as an example solution, it was still found to be difficult to standardize the measurement of specimens prone to out-of-plane curvature.

The interlaboratory study confirmed substantial size change (>10%) for several materials. The greatest size change typically occurred in the machine direction. In the interlaboratory study, several materials demonstrated shrinking in the machine direction, with corresponding expansion in the transverse direction. The measured results at the participating laboratories were found to be reproducible within ±5% of the absolute size change.

ACKNOWLEDGEMENTS

The authors are grateful to Dr. Michael Kempe, Dr. Sarah Kurtz, Dr. John Pern, and Stephen Glick of the National Renewable Energy Laboratory for their help/discussion with specimen fixturing, specimen handling, experimental methods, and other subsequent analysis. This work was supported by the U.S. Department of Energy under Contract No. DE-AC36-08GO28308 with the National Renewable Energy Laboratory and the National Institute of Standards and Technology of the U.S. Department of Commerce.

REFERENCES

[1] "ISO 11501 Plastics—Film and Sheeting—Determination of Dimensional Change on Heating," International Electrotechnical Commission: Geneva, 1–4 (1995).

[2] "ASTM D1204 - 08 Standard Test Method for Linear Dimensional Changes of Nonrigid Thermoplastic Sheeting or Film at Elevated Temperature," ASTM International, West Conshohocken, PA, 1–2 (2008).

[3] "ASTM D2732 - 08 Standard Test Method for Unrestrained Linear Thermal Shrinkage of Plastic Film and Sheeting," ASTM International, West Conshohocken, PA, 1–5 (2008).

[4] "ASTM C778 - 06 Standard Specification for Standard Sand," ASTM International, West Conshohocken, PA, 1–3 (2006).

[5] J.M. Moseley, D.C. Miller, Q.-U.-A.S.J. Shah, K. Sakurai, M.D. Kempe, G. Tamizhmani, and S.R. Kurtz, "The Melt Flow Rate Test in a Reliability Study of Thermoplastic Encapsulation Materials in Photovoltaic Modules," NREL/TP-5200-52586, 1–20 (2011).

[6] "IEC 62788-5 – Measurement Procedures for Materials Used in Photovoltaic Modules: Part 5 – Measurement of Change in Linear Dimensions of Sheet Encapsulation Material Under Thermal Conditions Plastics," International Electrotechnical Commission: Geneva, *(submitted)*.

[7] S.R.J. Axelsson, "On Soil Moisture mapping Using IR Thermography," Proc. ISPRS Cong., 27–38 (1988).

[8] "FLIR SC6XX Series User's Manual," FLIR Systems Inc.: Wilsonville, OR, 1–310 (2010).